AIRFRAME-INTEGRATED PROPULSION SYSTEM
FOR HYPERSONIC CRUISE VEHICLES*

3

Robert A. Jones and Paul W. Huber
NASA Langley Research Center

ABSTRACT

Research is underway on a new, hydrogen burning, airbreathing engine concept which offers good potential for efficient hypersonic cruise vehicles. Features of the engine which lead to good performance include; extensive engine-airframe integration, fixed geometry, low cooling, and the control of heat release in the supersonic combustor by mixed-modes of fuel injection from the combustor entrance. The engine concept is described along with results from inlet tests, direct-connect combustor tests, and tests of two subscale boilerplate research engines presently underway at conditions which simulate flight at Mach 4 and 7.

I. INTRODUCTION

It now appears certain that vehicles capable of repetitive long range flights in the atmosphere at hypersonic speeds can become a reality. How soon depends on the timing of the perfection and application of several areas of advanced technology - most especially those concerned with airbreathing propulsion and long-life, low-weight (actively-cooled) airframe structures and systems. This paper describes recent research on a totally airframe-integrated supersonic combustion ramjet (scramjet) which offers potential for efficient cruise propulsion at speeds from Mach 5 to 8. Regeneratively-cooled engine and actively-cooled airframe structure for hypersonic aircraft using the present propulsion concept are discussed in another paper in these same proceedings by Kelly, Wieting, Shore, and Nowak.

Most of the previous scramjet concepts that have been considered were of the "pod" type, capable of providing good internal performance but incapable of high installed thrust, due to the excessive cowl drag associated with the large nozzle expansions needed at high speeds. At speeds above Mach 4, practical considerations reduce the attractiveness of the pod approach. (See Fig 1). In addition to high external drag from the pressure force on the expanding cowl surface (necessary to obtain a suitable nozzle exit to inlet capture area ratio), the "pod" type engine installation suffers from insufficient capture area due to the inefficient use of cross section area of the flow within the vehicle shock layer. It also has drag increases and locally high heating rates due to flow interference between pods and vehicle. Variable geometry adds mechanical complexity and introduces significant weight penalties. The high internal contraction ratios and narrow annular passages typical of previous podded engines having good internal performance substantially increase cooling requirements to the point that more fuel might be needed to cool the engine than for combustion. This is particularly serious at the high Mach numbers where the fuel is required to cool certain parts of the airframe structure in addition to the engine. The design concept that has emerged from research at Langley emphasizes all three

major areas of concern: internal thrust minus total external drag, cooling requirements for the combined airframe and engine, and the total weight of airframe and engine. This airframe-integrated scramjet concept blends aircraft forebody and afterbody functions in combination with fixed geometry propulsion units utilizing a mixed mode of fuel injection.
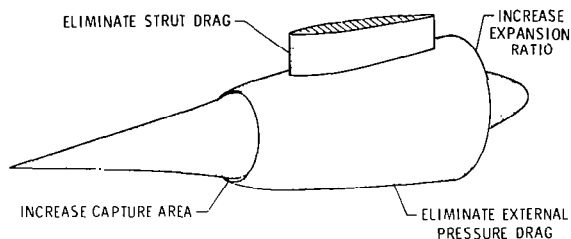

Figure 1. Improving "pod" Type Engine Performance

As illustrated in Figure 2, in order to obtain the required thrust at higher Mach numbers, the inlet area must be large enough to capture nearly all the airflow processed by the vehicle's undersurface bow shock. This suggests an annular inlet contiguous with the vehicle undersurface. Dividing the annular area into smaller rectangular units produces in effect a number of identical engine modules of a size and shape more nearly suited for ground tests.
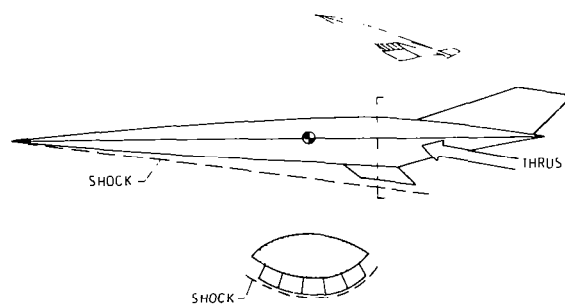

Figure 2. Scramjet-Vehicle Integration

Treating the engine in this way yields two important advantages: the vehicle's forebody performs a significant part of the inlet compression process, and its afterbody takes over a large part of the nozzle expansion. The engine design thus encompasses the entire undersurface of the vehicle. This approach has other drag-reducing advantages. The engine's external surfaces can easily be shaped to minimize installation losses by making

them parallel to the local flow, and the vehicle's base region can be used to continue the nozzle expansion process to the large exit to inlet area ratios required for efficient propulsion without incurring an excessive drag penalty.

This airframe-integrated scramjet concept has behind it extensive research on basic combustion and turbulent reaction flow processes, engine component configurations, and lightweight regeneratively-cooled structures. Two complete, subscale, research engines of heat sink structure are presently undergoing performance tests at conditions which simulate flight at Mach 4 and 7.

II. AIRFRAME-INTEGRATED MODULE

Inlet
       Subscale models of the fixed-geometry inlet have been tested under conditions simulating a flight Mach number range from 3 to 7 in conventional wind tunnels. This inlet has a rectangular capture area. (See Fig 3). The vehicle bow shock compresses flow in the vertical direction while the wedge-shaped inlet sidewalls compress the flow horizontally. This two-plane compression reduces the degree of change in the inlet flow field that occurs with changing flight speed or angle-of-attack and makes fixed geometry feasible. Sweep of the compression wedges and a cutback cowl provide spillage. This allows the inlet to start at low flight speeds. It also reduces the pressure gradient on the top surface to permit ingestion of the forebody boundary layer. Swept wedge-shaped struts at the throat complete the inlet compression process. These block about 60 percent of the flow cross section in the swept plane. In addition to making the inlet shorter, lighter, and lessening its cooling requirements, these struts also provide multiple planes for fuel injection; and therefore the mixing distance and the combustor are also shortened.
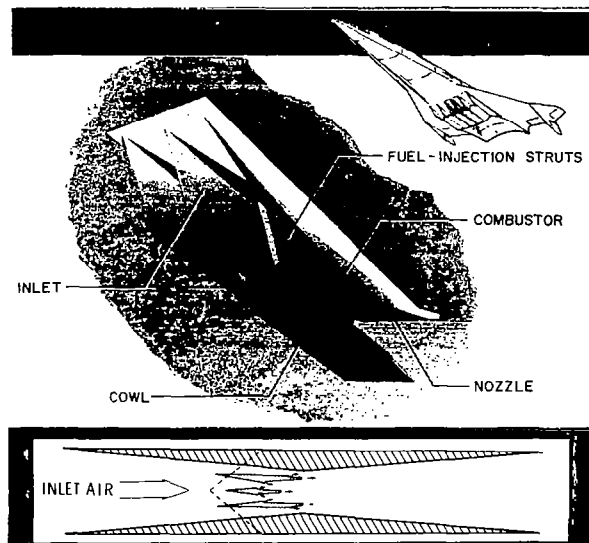
Figure 3. Airframe-Integrated Supersonic
Combustion Ramjet

Experimentally determined schedules for mass capture ratio, contraction ratio, and total pressure recovery (Fig 4) have shown this to be a practical, high-performance inlet concept.[1] The inlet starts easily for flight Mach numbers above 3, has a variable mass capture ratio with low loss spillage at the lower Mach numbers, and an aerodynamic contraction ratio that varies with Mach number in a desirable way. In addition to its low drag, cooling, and weight, it rivals variable-geometry inlets in aerodynamic performance. In fact, it has demonstrated a higher pressure recovery than previous variable-geometry inlets such as the NASA Hypersonic Research Engine (HRE).[2]
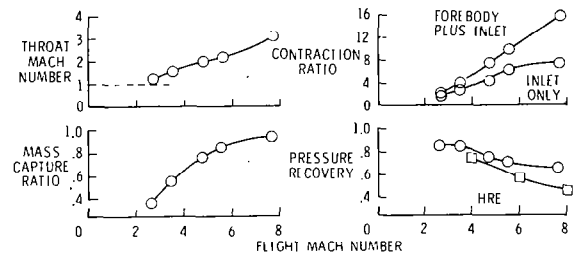
Figure 4. Inlet Aerodynamics

Combustor
       Over a period of several years, both analytical and experimental research has been conducted on the physics, thermodynamics, and physical means for injection, mixing, ignition, and combustion of hydrogen/air mixtures at locally supersonic speed and high enthalpy. From this effort has emerged a fuel injector-combustor concept which direct-connect tests have shown to provide a good combustion efficiency over a range of flight Mach numbers, and at the same time have low cooling and low structural-weight requirements.[3]

From this work has also come a unique mixed-fuel injection mode that allows effective control of the streamwise heat-release distribution over the Mach-number range (Fig. 5).
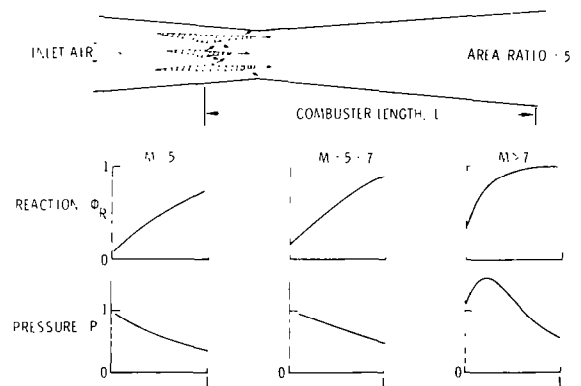
Figure 5. Combustor Operation

40

Dual-mode (subsonic/supersonic) combustion and minimum combustor length are obtained without necessity for additional fuel-injection stages (as required by previous concepts), which increase weight and cooling requirements. This is important because supersonic-combustion devices are sensitive to the distribution of heat release along the combustor flow length and its change with Mach number. For high propulsive efficiency, heat should be released as early in the combustor as possible (i.e.; higher pressure). At high flight speeds, fuel injected normal to the stream mixes, reacts, and releases its heat rapidly. At lower speeds, the large pressure rise associated with the rapid heat release can thermally choke the engine. At these lower speeds part of the fuel is injected parallel to the flow in the wake of the struts where it mixes and reacts much more slowly.

By proper apportionment of the fuel injected in the two modes, heat release can be tailored as desired. This combustor design also uses the struts to provide multiple in-stream planes for fuel injection. This in-stream fuel injection shortens the combustor length and lowers heat and skin friction losses compared to wall type fuel injectors. Combining these features, along with divergence of the combustor walls, yields efficient combustion performance over a wide Mach number range.

Nozzle
The flow into the nozzle is supersonic as there is no sonic throat. The after undersurface of the vehicle acts as the largest portion of the contoured nozzle wall. Essentially it is a half-nozzle, with only part of the dividing wall (partial cowl extension). The short cowl extension intercepts only a portion of the expansions from the contoured wall. At a Mach number of 6, about half the net thrust is generated by the large vehicle undersurface portion of the nozzle.

As a result of these factors, along with interactions between adjacent module wakes, spillage from the inlet, and nonuniform nozzle-entrance conditions, the nozzle plume has a highly 3-dimensional structure which changes with engine operating conditions, altitude, flight speed, vehicle attitude, etc. Furthermore, the nozzle flow analysis must account for multicomponent reacting species, shock, and viscous effects.
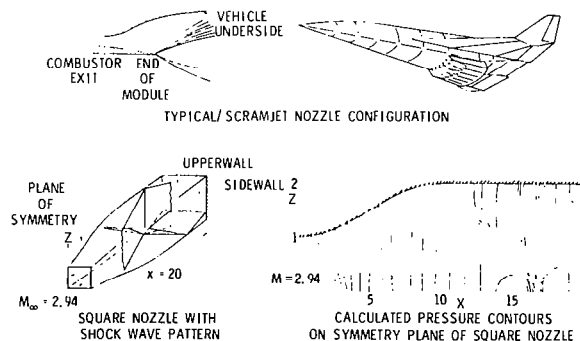
Because of this great complexity, it is necessary to employ a combination of lengthy computational methods[4] and experimental simulations[5] to approximate the nozzle flow structure. Figure 6 shows results of a nozzle computation.

III. SUBSCALE MODULE TESTS

The modular nature of the integrated scramjet engine provides certain inherent advantages for ground testing. For example, testing a single module can yield performance data representative of a wide range of engine sizes and thrust levels. The effects of the vehicle-forebody boundary layer on the ingested engine flow are readily simulated as to scale (the actual profiles depend on the particular forebody shape) by placing the engine so that it swallows the test facility nozzle boundary layer flow. Precompression by the vehicle's forebody bow shock can be simulated by testing at the flight enthalpy but at a Mach number reduced to account for the change in flow Mach number across the bow shock. In tests such as these it is not possible to include the large external nozzle of the vehicle afterbody (which provides about 50 percent of the net thrust at Mach numbers of 6 and above), but the installed performance (thrust minus drag) of the inlet-combustor module can be measured directly by supporting the model on a thrust balance.

To adequately verify engine performance over the design Mach number range, test data are needed at the higher Mach numbers where the fuel is injected primarily normal to the flow as well as the lower Mach numbers where the fuel is injected primarily parallel to the flow. To obtain such data, two subscale heat sink, research engine modules have been built. One is being tested at conditions simulating Mach 7 flight in an arc heated facility at Langley. The other is undergoing test at conditions simulating Mach 4 flight at the General Applied Sciences Laboratory (GASL) in New York. These engines are the same size, 20.3 cm by 16.3 cm (8 inch by 6.4 inch) inlet capture area and about 1.5 m (5 ft) in length and very similar in design. Both are heat sink designs intended for short duration tests of up to 20 seconds. Figure 7 shows the engine which is being used for Mach 7 tests prior to installation in the facility. It is made of copper with water-cooled leading edges for the sidewalls, the cowl, and the struts.
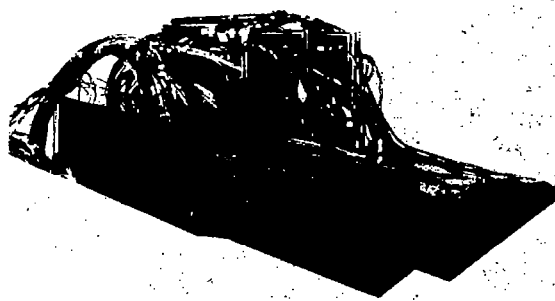

Figure 6. Integrated Scramjet Nozzle

Figure 7. Instrumented Subscale Scramjet Module

The Mach 4 engine is made of nickel. Both models are well instrumented internally with pressure orifices and heat transfer gauges. These research engines are designed for easy interchangeability of the fuel injection struts. The combustor area distribution near the fuel injectors can be varied by changing the struts or attaching pieces of different shape to downstream edges. Changes in downstream combustor area distribution can be simulated by air injection from the combustor sidewalls.

A schematic of the test setup in the Mach 7 facility is shown in figure 8 and a photograph of the facility with the research engine mounted in the test section is shown in figure 9. Note that the top wall of the engine model is positioned directly in line with the facility nozzle wall to swallow the facility boundary layer and thus simulate ingestion of the vehicle forebody boundary layer. A complete description of this arc-heated facility is given in Reference 6. It duplicates the Mach number, enthalpy and forebody boundary-layer conditions expected at the inlet for a vehicle at a flight Mach number of 7, but at dynamic pressure corresponding to only the very lowest values expected in flight, 16.8 kPa ($q_\infty \approx 350$ lb/ft^2).

- MEASUREMENT OF INSTALLED THRUST
- SIMULATES AIRCRAFT PRECOMPRESSION
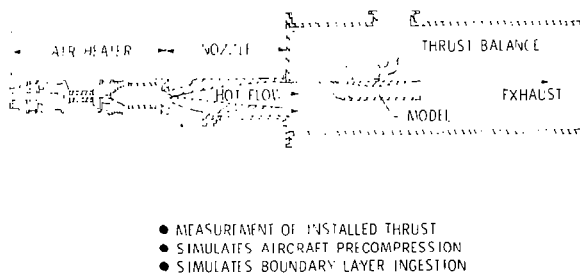- SIMULATES BOUNDARY LAYER INGESTION

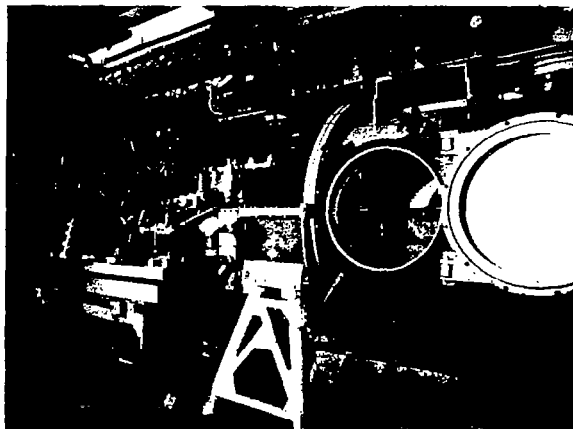Figure 8.   Schematic of Mach 7 Scramjet Test Facility

Figure 9.   Mach 7 Scramjet Test Facility

The Mach 4 test setup at GASL is similar in that it duplicates the Mach number and enthalpy and forebody boundary-layer conditions expected at the inlet for a vehicle at a flight Mach number of 4. However, the facility heater is of the combustion type. Hydrogen and air are burned in the stagnation chamber and oxygen is added to replace that used for burning so that the test gas stream contains water-vapor as well as nitrogen and oxygen.

Preliminary tests in both facilities have been made in which hydrogen was burned in the engine. In these preliminary tests the modes of fuel injection and the split between parallel and perpendicular injection were varied, different strut geometries were tested, and various amounts of air were injected from the combustor sidewalls to change effective area distribution. No ignitors were used - spontaneous ignition was relied upon. As might be expected in the first tests of a new scramjet concept, these initial parametric tests uncovered a whole range of problems. These included facility-model interactions in which fuel injection caused test cabin pressure to increase, with subsequent inlet unstart (this problem has now been solved), cases where ignition did not occur at all in the engine, and cases where combustion heat release caused the inlet to unstart. There were also cases where combustion was achieved in the engine with no apparent interaction in the inlet, and measured internal thrust levels close to the predicted values were obtained.

Some of the results from one of the more successful of these preliminary tests in the Mach 7 facility are shown in Figure 10. For this test the total enthalpy of the flow approaching the inlet was 2.6 MJ/kg (1128 Btu/lb) with a total pressure of 30 atmospheres simulating a flight condition of Mach 7 at an altitude of 35 km (115,000 ft). Estimates using the method of Reference 7 with the reaction rate correlation of Reference 8 indicate that for stoichiometric fuel-air ratios at the low pressure of these preliminary Mach 7 tests only 20 percent of the fuel reacts. Therefore air equal to about 7 percent of that captured by the inlet was injected from the sidewalls to decrease the effective cross sectional area further downstream in the combustor, raise static pressure, and thus increase the reaction efficiency. Hydrogen fuel was injected from the struts normal to the flow at a fuel equivalence ratio of 0.5 and the drag and internal pressures measured (solid symbols in Figure 10). Note the large increase in pressure due to combustion which begins just downstream of the fuel injection location. The internal thrust obtained from the difference in balance readings with and without fuel was 225 N (50.6 lb). An estimate of the change in force due to internal pressures was made by interpolating for pressure between orifice locations and integrating over the entire internal surface of the engine. This integration gave a value of approximately 351 N (79 lb) but, of course, internal shear forces which act in the drag direction were not included.

From the change in measured heating rate in the combustor with and without fuel and the use of a correlation method of Orth and Billig,[9] the overall reaction efficiency (percentage of available fuel actually reacted) was estimated to be

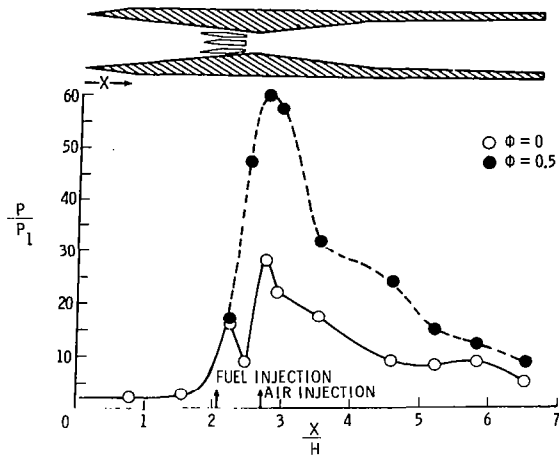69 percent; since the injected equivalence ratio was 0.5, this gave a reacted fuel equivalence ratio of 0.34.

Figure 10. Internal Sidewall Pressure Distribution (Mach 7 Flight Simulation)

Figure 11. Predicted Internal Thrust

A comparison of the measured internal thrust with predictions based on simple one-dimensional theory[7,8] as a function of reaction efficiency is given in Figure 11. The solid line represents a real gas calculation assuming zero chemical reaction time (equilibrium) and no air injection from the combustor sidewalls. The fuel is assumed to react completely as soon as it is mixed (mixing controlled combustion) and an empirical relation for mixing as a function of flow length is used. The assumption of instantaneous reaction becomes inappropriate for low pressure levels. Because of the present low dynamic pressure conditions of the Mach 7 facility, 16.8 kPa (350 lb/ft^2) or about one-third of the design operating condition of the engine), the combustion process appears to be significantly affected by the finite time required for chemical reactions as well as the mixing rate. The use of air injection from the combustor sidewalls was employed to increase the pressure in the initial combustion region. The method of Reference 7 was modified to account for sidewall air injection and finite chemical reaction rates using the correlation for non-equilibrium hydrogen-air reactions of Pergament.[8] These results are shown as open symbols in Figure 11 for various ratios of injected air mass flow to inlet capture mass flow.

The results of the preliminary parametric tests made to date indicate that the inlet-combustor interactions experienced at large fuel-air ratios can be solved with minor geometric changes in the region of the fuel injector struts and that the reaction-rate limited combustion can be solved by increasing the operating pressure of the facility. Furthermore, the agreement between experimental results obtained so far and the theoretical performance predictions lends credence to the predictions of overall performance (thrust, specific impulse, and cooling requirement) of this airframe-integrated scramjet concept.
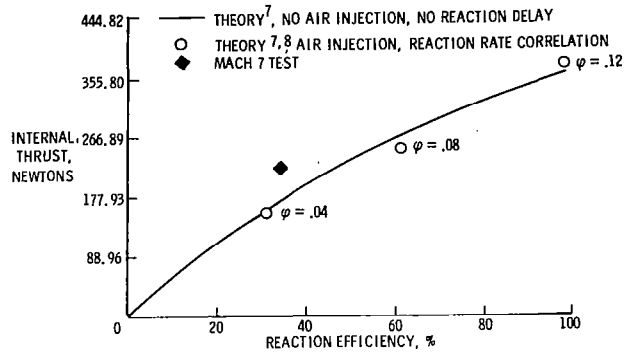
IV. PREDICTED PERFORMANCE CHARACTERISTICS

As a result of the large background of research compiled on components of the airframe-integrated scramjet, reasonable estimates can be made of the installed module performance (C_T and I_{sp}), module and system weights, module cooling requirements, and flight characteristics of an airframe-integrated scramjet vehicle.

It is interesting to compare the predicted specific impulse of the integrated scramjet with other high-speed propulsion systems. Figure 12 shows the fuel specific impulse for turbojets, ramjets, scramjets, and rockets as a function of the flight Mach number for hydrocarbon (JP) and hydrogen (H_2) fuel. The H_2-fueled scramjet at Mach 6 has a higher specific impulse than the JP-fueled turbojet at Mach 2. No real competitor to the scramjet exists at Mach numbers greater than about 6, even for an on-design cruise application.
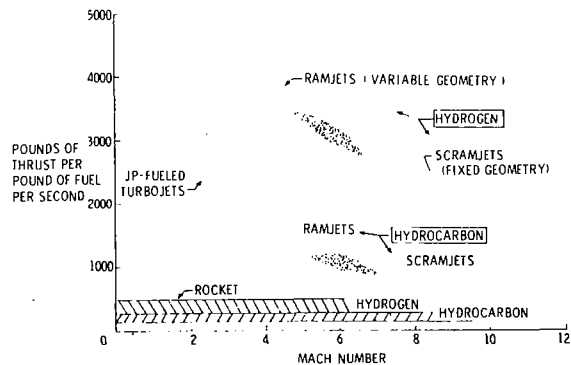

Figure 12. Propulsion Options

Installed Thrust

It is obviously not possible to define installed engine performance independent of vehicle characteristics. The vehicles forebody length, shape, and surface have a marked influence on the boundary layer and flow distribution entering the engine inlet, while the afterbody geometry strongly

43

influences nozzle expansion, as previously discussed. Here for simplicity, we treat scramjet performance of a "nominal" forebody and afterbody, along with suggested means to estimate effects on performance due to departures from the "nominal." We distinguish installed from internal performance by accounting for several external effects chargable to the engine. These include additive (or spillage) drag forces, cowl drag forces, effects of ingested forebody boundary layer on entering mass, energy and momentum, frictional and heat-transfer losses, and effects in the flight direction of normal forces on the capture flow and exhaust plume (since the coordinate system for thrust calculation goes in the forebody, or engine-flow, direction). Pinckney[10] has given a description of the complete performance calculation method, along with numerical results as functions of the various dependent parameters. Figure 13 shows thrust coefficient (C_T) and specific impulse (I_{sp}) as functions of fuel-air equilivance ratio (φ) and flight Mach number (M_∞) for the "nominal" vehicle underbody. The values of C_T and I_{sp} are for a dynamic pressure of 23.9 kPa (500 lb/ft²) but are applicable to other altitudes as long as the reactions are controlled by mixing. The crossing of the curves is a result of different splits between parallel and normal fuel injection used to avoid thermal choking below Mach 6 and to reduce combustor heat load at Mach 8.
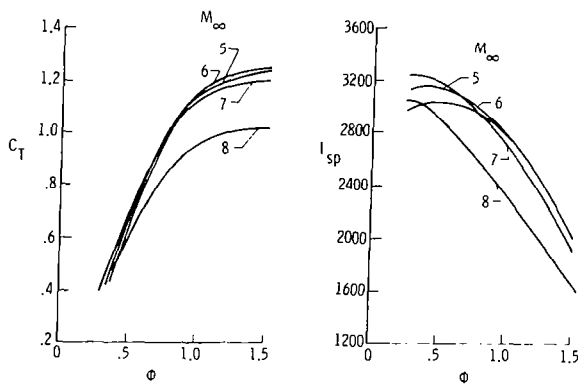

Figure 13. Scramjet Installed Performance

Although not shown, the installed performance also varies as a function of the precompression achieved by the vehicle forebody. The thrust coefficient increases with increasing forebody flow deflection angle due to the increased mass flow entering the inlet until an angle of about 12 degrees. Above 12 degrees the thrust decreases due to the overriding influence of the increasing normal-force component in the flight direction. While the installed engine performance includes external effects chargeable to the engine such as spillage, cowl drag, and effects of ingesting the forebody boundary layer, it does not include the aircraft drag. When vehicle drag is included, the peak thrust minus drag of the total system occurs at forebody flow deflection angles near 7 1/2 degrees for configurations optimized to cruise at Mach 6.

Forebody boundary-layer ingestion by the inlet represents one of the more important non-ideal flow effects on installed scramjet performance. Defects in entering mass flow due to the boundary-layer displacement show up directly as thrust decrements, while defects in entering momentum also degrade the performance. However, the loss in performance associated with ingesting the forebody boundary layer is less than the drag increase associated with diverting this flow or mounting the engine on a pylon. To account approximately for forebody boundary layers different from the "nominal" case cited, the thrust should be changed in proportion to the change in mass flow entering the inlet (due to change in boundary-layer-displacement thickness).

The forebody-boundary-layer characteristics used in determining the scramjet performance in Figure 13 are based on flat-plate flow of 12.2 m (40 ft) length and 667 K (1200°R) surface temperature. Transition was assumed to occur at $R_\theta = 10^3$ (momentum thickness Reynolds number). It is interesting that the ingested boundary-layer thickness, and hence thrust decrement, can be reduced by cooling the forebody. The energy loss to the cold wall can be recovered in the regenerative heating process (higher fuel T). The nozzle area ratio (engine nozzle exit to cowl) used in the calculations was about 3.6, and the external surface of the cowl lip was inclined 3 degrees to the forebody surface. The cowl drag forces amounted to about 5 percent of the thrust.

The influence of afterbody geometry (nozzle expansion) on the thrust coefficient is illustrated in Figure 14. Values of C_T as functions of nozzle expansion angle (ε) and length (L_N/H_C) for Mach 6 and a fuel equivalence ratio of 1.0 are shown. For expansion angles in the range of 16 to 24 degrees, thrust coefficient is primarily sensitive to the nozzle length (area ratio) up to values of about 4 H_C (module cowl height).
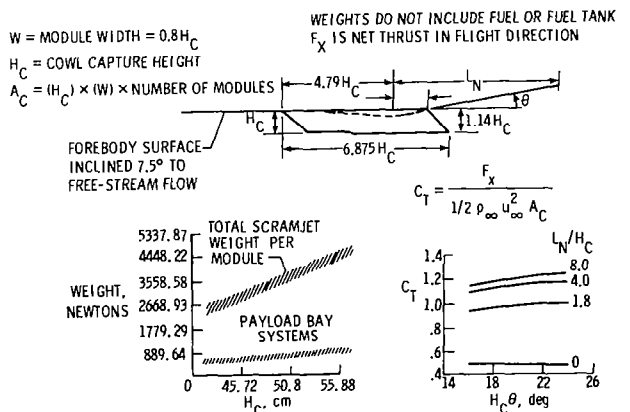

Figure 14. Scramjet Weight and Nozzle Geometry

Engine Weight

Detailed estimates of scramjet engine module weights and weights of the associated subsystems have been made based on both in-house and contractual structural[11] and system studies, including

44

results from the HRE flight-weight regeneratively-cooled engine program. Figure 14 shows variation of module and systems weight as a function of the module cowl height, H_C. This case assumes a six-module scramjet engine of 4.1 kg/sec (9 lb/sec) hydrogen flow (maximum fuel flow rate for this study) which corresponds to $\phi = 1.5$ operation at $q_\infty = 71.8$ kPa (1500 lb/ft^2) and $M_\infty = 6$.

For illustration, the weight breakdown for the case of six 45.7 cm (18 in.) high modules would be as follows: in-board engine modules, 236 kg (520 lb) each; outboard engine modules, 259 kg (570 lb) each, where both numbers include the engine subsystems (controls, valves, plumbing, and instrumentation); other subsystems, total 279 kg (615 lb). These weights average out, per module, to 290 kg (639 lb) total (engine and subsystems) and 47 kg (103 lb) for the other subsystems. The weight of hydrogen fuel and tankage would be additional.

Engine Cooling Requirements

Detailed computations of the heat-transfer rates and resulting cooling requirements for the component sections of the scramjet module have been made and compared with the available heat sink in the hydrogen fuel (also used as a coolant). The results depend strongly, of course, upon the assumptions of allowable wall and fuel temperature, type of material, coolant flow path, etc

Figure 15 shows the heat load for various engine module components as a percentage of the available heat sink in the hydrogen fuel as it flows to the combustor at an equivalence ratio of 1.0 for flight at Mach 6 and $q_\infty = 23.9$ kPa (500 lb/ft^2). For this condition, the total cooling required by the engine is about 50 percent of the available fuel heat sink.[11] The excess cooling available could be used to cool portions of airframe structure.
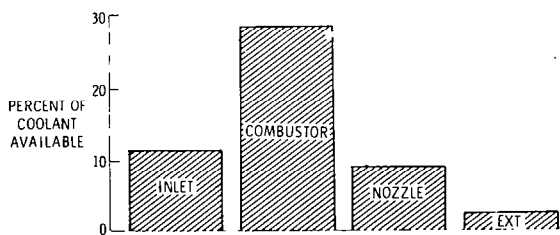

Figure 15. Engine Heat Load; $M_\infty = 6$, $q_\infty = 23.9$ kPa (500 lb/ft^2).

V. CONCLUDING REMARKS

Based on the concept of total engine-vehicle integration, the present scramjet concept appears to be capable of providing efficient airbreathing propulsion at Mach number of 5 and higher. We conclude this airframe-integrated scramjet concept has the potential for high thrust and efficiency, low drag and weight, low cooling requirement with excess cooling available to cool airframe components, and application to a wide range of vehicle sizes.

VI. REFERENCES

1. Trexler, C. A.: Inlet Performance of the Integrated Langley Scramjet Module. AIAA Preprint No. 751212, Sept. 1975.

2. Staff, AiResearch: Hypersonic Research Engine Project Phase II Aerothermodynamics Integration Model Development. Final Technical Data Report. NASA CR-132654, May 1975.

3. Henry, J. R.; and Anderson, G. Y.: Design Considerations for the Airframe-Integrated Scramjet, NASA TM X-2895, Dec. 1973.

4. Dash, S. M.; and Del Guidice, P. D.: Numerical Methods for the Calculation of Three-Dimensional Nozzle Exhaust Flow Fields. NASA SP-347, Part I, Mar. 1974.

5. Cubbage, J. M.; Talcott, N. A., Jr.; and Hunt, J. L.: Scramjet Exhaust Simulation for Hypersonic Aircraft Nozzle Design and Aero Model Tests. AIAA Preprint No. 77-82, Jan. 1977.

6. Boatright, W. B.; Sabol, A. P.; Sebacher, D. J.; Pinckney, S. Z.; and Guy, R. W.: Langley Facility for Tests at Mach 7 of Subscale, Hydrogen Burning, Airframe-Integrated, Scramjet Models. AIAA Preprint No. 76-11, Jan. 1976.

7. Anderson, G. Y.: An Examination of Injector/Combustor Design Effects on Scramjet Performance. 2nd International Symposium on Air-Breathing Engines, Sheffield, England, Mar. 25-29, 1974.

8. Pergament, H. S.: A Theoretical Analysis of Non-equilibrium Hydrogen-Air Reactions in Flow Systems. AIAA-ASME Paper No. 63-113, Apr. 1963.

9. Orth, R. C.; Billig, F. S.; and Grenleski, S. E.: Measurement Techniques for Supersonic Combustion Testing. Instrumentation for Air-breathing Propulsion Progress in Astronautics and Aeronautics, vol. 34, 1973.

10. Pinckney, S. Z.: Internal Performance Predictions for the Langley Scramjet Engine Module. NASA TM X-74038, Jan. 1978.

11. Killackey, J. J.; Katinszky, E. A.; Tepper, S.; and Vuigner, A. A.: Thermal-Structural Design Study of an Airframe-Integrated Scramjet. NASA CR-145368, June 1978.